Noise-induced transitions in a generalized logistic model with delay

Irina A. Bashkirtseva
Irina.Bashkirtseva@urfu.ru

Ekaterina D. Ekaterinchuk
Ek.Ekaterinchuk@gmail.com

Lev B. Ryashko
lev.ryashko@urfu.ru

Department of Theoretical and Mathematical Physics,
Institute of Natural Sciences and Mathematics,
Ural Federal University (Yekaterinburg, Russia)

Abstract

The stochastic phenomena in the generalized randomly forced logistic model with delay is considered. The probabilistic mechanisms of the noise-induced transitions between coexisting attractors, and between separate parts of the unique attractor are studied. For the analysis of these phenomena, a new semi-analytical approach is suggested. Our method takes into account a geometry of the mutual arrangement of attractors, their basins of attraction, and corresponding confidence domains. Constructive abilities of this approach are demonstrated for the various parametric zones of the generalized logistic model with delay.

1 Introduction

One of the challenging problems of the modern nonlinear dynamics and its applications is a clarification of the underlying reasons of stochastic phenomena in nonlinear dynamical systems. An interplay between nonlinearity and stochasticity may lead to unexpected after-effects, such as stochastic resonance [16], noise-induced transitions [11, 1], noise-induced "chaos-order"transformations [8, 10], and stochastic bifurcations [2]. These phenomena have been found and actively investigated in various domains of science.

An important stage in the investigation of these stochastic effects is a study of their intrinsic mechanisms on the base of adequate conceptual models. The one-dimensional discrete logistic model is one of the first examples [17] demonstrating how due to nonlinearity a simple difference equation can generate a variety of dynamic regimes, both regular (equlibria, cycles) and chaotic [22].

Development of methods for the analysis of many nonlinear stochastic effects was also initiated and carried out on the basis of this model [19, 7]. Various extended versions of the logistic model play an important role in the theoretical development of nonlinear dynamics [9, 15, 26, 23, 3, 20] . The logistic model with delay [23] should be noted here especially. This model, along with the classic regular attractors such as equilibria and discrete cycles, exhibits attractors in a form of close invariant curves that appear as a result of the Neimark-Sacker (NS) bifurcation [25]. Dynamics of this two-dimensional deterministic model was studied in [24, 21, 18].

In present paper, we consider a generalized version of the logistic model with delay. Our aim is to study, on the example of this model, the probabilistic mechanisms of noise-induced transitions between coexisting attractors.

In: A.A. Makhnev, S.F. Pravdin (eds.): Proceedings of the International Youth School-conference «SoProMat-2017», Yekaterinburg, Russia, 06-Feb-2017, published at http://ceur-ws.org

Nonlinear systems with stochastic phenomena can be revealed and demonstrated by direct numerical simulations of the random solutions. However, for the detailed parametric analysis and clarification of the underlying mechanisms, analytical tools are required. A comprehensive mathematical description of stochastic dynamics in discrete systems with random perturbations is given by Perron-Frobenius equation [12, 14]. An analytical solution of this functional equation, even in the one-dimensional case, is possible only for very particular examples. In these circumstances, semi-analytical approximations are very useful. In [4, 5], the stochastic sensitivity functions (SSF) technique has been proposed for the analysis of randomly forced equilibria, discrete cycles and closed invariant curves. On the base of SSF technique, approximations of the probabilistic distribution around attractors of discrete systems can be obtained in a form of confidence domains.

In present paper, we show how noise-induced phenomena can be studied parametrically by means of the geometric analysis of the mutual arrangement of attractors, their basins of attraction, and corresponding confidence domains. Our approach is universal, but here is carried out on the conceptual example of the generalized logistic model with delay.

In Section 2, we give an overview of dynamical regimes and bifurcations for the deterministic generalized logistic model with delay. Parametric zones of stable equilibria, discrete cycles and closed invariant curves are determined. Here, two scenarios of the loss of stability of the equilibrium with a birth of the stable closed invariant curve (NS- bifurcation), or with a birth of the discrete 4-cycle are discussed. The phenomenon of coexistence equilibria and three Feigenbaum trees are demonstrated.

In Section 3, we study how random noise affects the attractors of the model under consideration. On the base of SSF technique, it is shown how to construct confidence domains for the description of the spatial distribution of random states around equilibria, 4-cycles, and closed invariant curves. A detailed parametric analysis of the stochastic sensitivity of attractors is carried out. Noise-induced transitions between coexisting attractors, and also between separate parts of the unique attractor are studied. Here, we focus on the analysis of the stochastic transitions "4-cycle $\to$ equilibrium "invariant curve $\to$ 4-cycle" in zones of bistability, and "closed invariant curve $\to -\infty$"in the zone of monostability.

2 Deterministic model

Consider a generalized logistic model with delay

$$x_{t+1} = \mu x_t (1 - \alpha x_t - \beta x_{t-1}), \tag{1}$$

where x_t is a density of the population at time t, parameters μ, α, and β are positive, and $\alpha + \beta = 1$.

The equation (1) can be transformed to the following system

$$\begin{aligned} x_{t+1} &= \mu x_t (1 - (1-\beta) x_t - \beta y_t) \\ y_{t+1} &= x_t. \end{aligned} \tag{2}$$

The system (2) possesses two equilibria $M_0(0,0)$ and $M_1\left(\frac{\mu-1}{\mu}, \frac{\mu-1}{\mu}\right)$. The non-trivial equilibrium M_1 exists for $\mu > 1$ and does not depend on β.

For system (2), the Jacobi matrix can be written as

$$F = \begin{bmatrix} \mu - 2\mu(1-\beta)x - \mu\beta y & -\mu\beta x \\ 1 & 0 \end{bmatrix}.$$

For equilibria M_0 and M_1, corresponding Jacobi matrices have the following representation:

$$F_0 = \begin{bmatrix} \mu & 0 \\ 1 & 0 \end{bmatrix}, \qquad F_1 = \begin{bmatrix} \mu - (\mu-1)(2-\beta) & \beta(1-\mu) \\ 1 & 0 \end{bmatrix}.$$

The matrix F_0 has eigenvalues $\lambda_1 = 0, \lambda_2 = \mu$, therefore, the equilibrium M_0 is stable for $0 < \mu < 1$. For the equilibrium M_1, the characteristic equation can be written in the following form:

$$\lambda^2 - S\lambda + J = 0, \tag{3}$$

where $S = \mu - (\mu-1)(2-\beta),\ J = \beta(\mu-1)$.

Bifurcations of two-dimensional maps are traditionally shown in the plane (S, J) by a so-called "stability triangle". Sides of this triangle are defined by the following equations: $1 - S + J = 0$ for the fold bifurcation, $1 + S + J = 0$ for flip (period-doubling) bifurcation, and $J = 1$ for Neimark-Sacker bifurcation.

In the plane (β, μ), corresponding lines are $\mu = 1$, $\mu = \frac{2\beta-3}{2\beta-1}$, and $\mu = 1+\frac{1}{\beta}$. Taking into account the additional condition $0 \le \beta \le 1$, for the equilibrium M_1 we have a "stability pentagon".

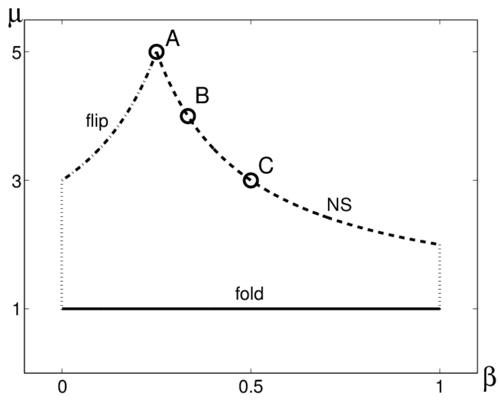

Figure 1: "Stability pentagon" for the equilibrium M_1.

For the "stability pentagon" shown in Fig. 1, solid, dash-dotted, and dotted lines correspond to fold bifurcation, flip bifurcation, and Neimark-Sacker bifurcation, respectively.

Consider details of the emergence of the Neimark-Sacker bifurcation. For the equilibrium M_1, the characteristic equation (3) has a pair of complex eigenvalues $\lambda_{1,2} = \eta(\beta,\mu)e^{\pm i\theta(\beta,\mu)}$, where

$$\eta(\beta,\mu) = \sqrt{\beta(\mu-1)}, \qquad \theta(\beta,\mu) = \arctan \frac{\sqrt{4\beta(\mu-1) - (\mu - (\mu-1)(2-\beta))^2}}{\mu - (\mu-1)(2-\beta)}.$$

At the points of the Neimark-Sacker bifurcation, it holds that

$$\theta = \arctan \frac{\sqrt{4\beta - 1}}{2\beta - 1}, \quad -\frac{\pi}{2} < \theta < \frac{\pi}{2}, \quad \eta(\beta,\mu) = 1.$$

Conditions of the occurrence of the Neimark-Sacker bifurcation are following [13]:

$$\eta'_\beta(\beta,\mu) \ne 0, \quad \eta'_\mu(\beta,\mu) \ne 0 \tag{4}$$

$$e^{i\theta k} \ne 1, \quad k = 1, 2, 3, 4. \tag{5}$$

The condition (4) is always satisfied. The inequality (5) implies the restrictions $\beta \ne 0.25$, $\beta \ne \frac{1}{3}$, $\beta \ne 0.5$ marked in Fig. 1 by points A, B, and C, respectively. In present paper, we focus on the study of system (1) near $\beta = 0.5, \mu \in (0, 3.3)$ and $\beta = \frac{1}{3}, \mu \in (0, 4.2)$.

As typical values of the parameter β, we have chosen $\beta = 0.49$, $\beta = 0.5$, and $\beta = 0.51$ и $\beta = 0.32$. In Fig. 2, for these parameter values, attractors of system (2) are plotted versus μ. In Fig. 2a for $\beta = 0.51$, one can see equilibria, closed invariant curves, discrete cycles, and chaotic attractors. As the parameter μ increases, the equilibrium M_1 loses its stability, and closed invariant curve appears as a result of the Neimark-Sacker bifurcation. With further increasing μ, the closed invariant curve expands, becomes non-smooth, and collapses before being transformed to the discrete cycle. For $\beta = 0.51$, a variety of attractors and bifurcations is the same as for the case β=1 considered in detail in [6].

For $\beta = 0.5$, a loss of the stability of the equilibrium M_1 implies an appearance of the discrete 4-cycle. As one can see in Fig. 2b, for $\beta = 0.5$, the system has only two types of attractors, namely the equilibrium and 4-cycle. Note that for $\beta = 0.5$ and $\beta = 0.51$ the system is monostable. In Fig. 2c, it can be seen that for $\beta = 0.49$ the system has three types of attractors, namely the equilibrium, 4-cycle, and closed invariant curve. Moreover, there exists an interval of the bistability $3.03917 \le \mu \le 3.065$ where the closed invariant curve coexists with 4-cycle which appears at $\mu = 3.03917$. These attractors have corresponding basins of attraction in the plane xOy.

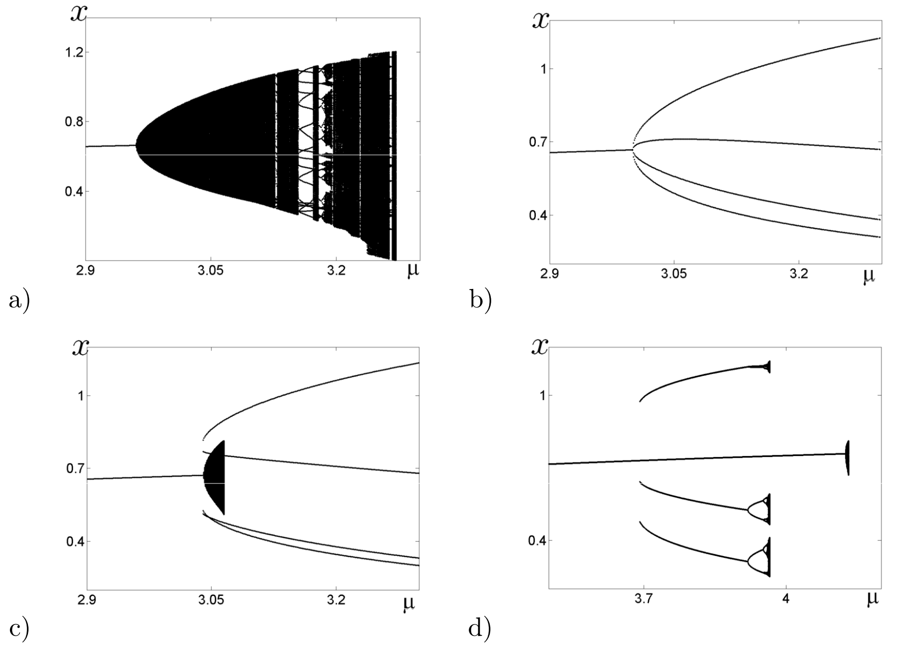

Figure 2: Attractors of system (2) for $\beta = 0.51$ (a), $\beta = 0.5$ (b), $\beta = 0.49$ (c) and $\beta = 0.32$ (d).

In Fig. 2d, for $\beta = 0.32$, one can see equilibria, closed invariant curves, discrete cycles, and chaotic attractors. Moreover, there exists an interval of the bistability $3.6889 \leq \mu \leq 3.966$ where the equilibrium coexists with three Feigenbaum trees. For $\beta = 0.32$, a saddle-node bifurcation of the birth of the 3-cycle occurs at $\mu = 3.6889$.

Consider in detail the stability of attractors of system (2) for $\beta = 0.49$ and $\beta = 0.32$.

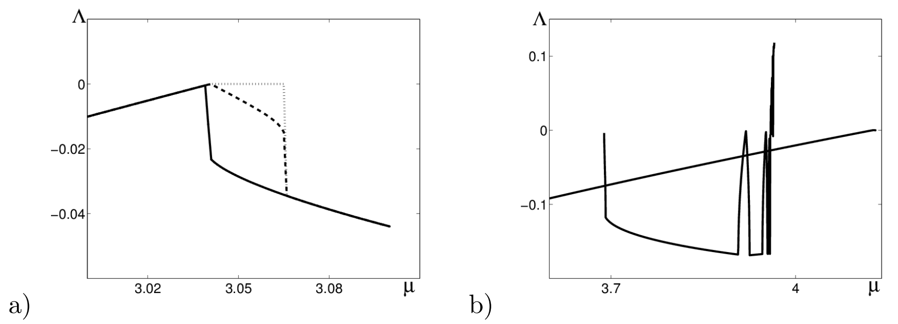

Figure 3: Lyapunov exponents are plotted for $\beta = 0.49$ a), $\beta = 0.32$ b).

In Fig. 3a, Lyapunov exponents for $\beta = 0.49$ versus parameter μ are shown. For the closed invariant curve, plotted are largest (dotted line) and minor (dashed line) Lyapunov exponents, and only largest one (solid line) for the discrete cycle. In bifurcation points and in the zone of closed invariant curves, the largest Lyapunov exponents are zero. It can be noted that in the zone of bistability, 4-cycle is more stable than the closed invariant curve.

In Fig. 3b, Lyapunov exponents for $\beta = 0.32$ versus parameter μ for the equilibrium and three Feigenbaum trees are shown (solid line). In bifurcations of the period-doubling the largest Lyapunov exponents are zero. As the parameter μ increases discrete cycles increase their stability with respect to equilibrium. Positive values of the Lyapunov exponent indicate chaotic regimes.

3 Stochastic model

Consider now a stochastically forced system (2):

$$\begin{aligned} x_{t+1} &= \mu x_t(1 - (1-\beta)x_t - \beta y_t) + \varepsilon \xi_t \\ y_{t+1} &= x_t. \end{aligned} \tag{6}$$

Here, ξ_t are uncorrelated standard Gaussian random values with parameters $\mathrm{E}\xi_t = 0$, $\mathrm{E}\xi_t^2 = 1$, the value ε is a noise intensity.

In presence of noise, the deterministic attractor is blurred. Near bifurcation points, a dispersion of random states increases. To study these noise-induced phenomena, we consider in detail how noise impacts on the attractors. For the constructive description of the dispersion of random states near attractors, we will use the stochastic sensitivity functions technique and method of confidence bands.

3.1 Analysis of stochastically forced equilibria

Consider an influence of noise on the equilibria M_0 and M_1 in zones where they are stable. Stochastic sensitivity matrices W_0 and W_1 of equilibria M_0 and M_1, correspondingly, can be found analytically [4]:

$$\begin{aligned} W_0 &= \frac{1}{(1-\mu^2)} \begin{bmatrix} 1 & \mu \\ \mu & 1 \end{bmatrix}, \\ W_1 &= \frac{1}{(\mu-1)(\mu-\beta(\mu-1)^2+2\beta^2(\mu-1)^2-3)} \begin{bmatrix} -1+\beta-\beta\mu & -2+\beta+\mu-\mu\beta \\ -2+\beta+\mu-\mu\beta & -1+\beta-\beta\mu \end{bmatrix}. \end{aligned} \tag{7}$$

Eigenvectors of these matrices specify main directions of deviations, and eigenvalues define a size of deviations in these directions. Note that matrices (7) have the same eigenvectors which do not depend on the parameters β and μ: $u_1 = (-1,1)^\top$, $u_2 = (1,1)^\top$.

Eigenvalues $\eta_{0,1}, \eta_{0,2}$ of the matrix W_0, and eigenvalues $\eta_{1,1}, \eta_{1,2}$ of the matrix W_1 are written as

$$\eta_{0,1} = \frac{1}{1-\mu}, \qquad \eta_{0,2} = \frac{1}{1+\mu},$$

$$\eta_{1,1} = \frac{1}{(1-\mu)(\beta\mu-\beta-1)}, \quad \eta_{1,2} = \frac{1}{3+\beta(\mu-1)^2-2\beta^2(\mu-1)^2-\mu}.$$

These eigenvalues play a role of the scalar characteristics of the stochastic sensitivity of the equilibria M_0 and M_1. Note that approaching bifurcation values $\mu = 1$ for M_0, and $\mu = 3.0408$ for M_1, where these equilibria become unstable, the stochastic sensitivity tends to infinity.

In Fig. 4a, eigenvalues $\eta_{1,1}$, $\eta_{1,2}$ ($\eta_{1,1} > \eta_{1,2}$) of the matrix W_1 are plotted versus parameter μ for $\beta = 0.49$.

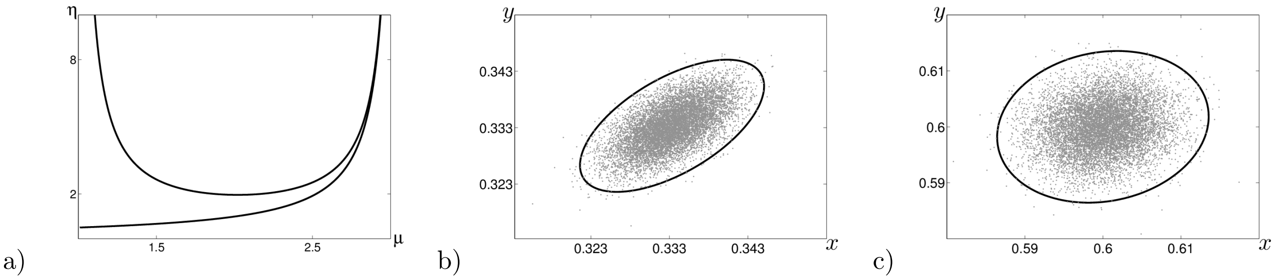

Figure 4: Stochastic system (6) with $\beta = 0.49$: a) eigenvalues of the stochastic sensitivity matrix of the equilibrium M_1; b) random states (dots) and confidence ellipse for $\varepsilon = 0.003$, $\mu = 1.5$; c) random states and confidence ellipse for $\varepsilon = 0.003$, $\mu = 2.5$.

In Fig. 4b,c, plotted are random states of system (6) for the noise intensity $\varepsilon = 0.003$ and two values of the parameter $\mu = 1.5$ and $\mu = 2.5$. These random states were found by the direct numerical simulation of solutions of the stochastic system (6). It can be noted that with increasing μ the dispersion of random states grows. This is consistent with the changes in the stochastic sensitivity in Fig. 4a. In Figs. 4b,c, along with random states, confidence ellipses found by the stochastic sensitivity function technique are plotted. As can be seen, these ellipses adequately reflect a configuration of random states found numerically.

3.2 Noise-induced transitions

Applying techniques of stochastic sensitivity functions give opportunities to describe noise-induced transitions between attractors. At first consider noise-induced transitions in stochastic system (6) with $\beta = 0.49$ in zones of the bistability.

In Fig. 5ab, numbered elements $\{(\bar{x}_1, \bar{y}_1), \dots, (\bar{x}_4, \bar{y}_4)\}$ of the deterministic 4-cycle of system (2) with $\mu = 3.04$ are plotted by asterisks, and random states of system (6) for noise intensity $\varepsilon = 0.0005$ (a), and $\varepsilon = 0.001$ (b) are plotted by dots.

As can be seen, random states are dispersed near states of 4-cycle in different ways. Using an algorithm one can construct stochastic sensitivity matrices and confidence ellipses around four states of the cycle. In Fig. 5ab, confidence ellipses are plotted along with random states. As can be seen these ellipses well reflect a dispersion of random states.

For $\mu = 3.04$, the deterministic system possesses two coexisting attractors, namely an equilibrium and 4-cycle. In Fig. 5ab, shown are basins of attraction of the equilibrium (dark grey) and 4-cycle (light grey).

For weak noise, random states are slightly dispersed near points of the deterministic cycle, and noise-induced transitions do not occur. This also can be seen from the mutual arrangement of confidence ellipses (white curves) and borders of the basins of attraction: small ellipses entirely belong to the basin of attraction of 4-cycle (see Fig. 5a). With increasing noise, these ellipses expand, and cross the border of the basin of attraction. This fact signals about the onset of noise-induced transitions from the basin of attraction of the 4-cycle to the basin of attraction of the equilibrium (see Fig. 5b).

Consider how eigenvalues of the stochastic sensitivity matrices depend on the parameter μ for $\beta = 0.49$. In Fig. 5c, plotted are largest eigenvalues of the stochastic sensitivity matrices of different states of 4-cycle. As one can see, the stochastic sensitivity decreases with growth of μ.

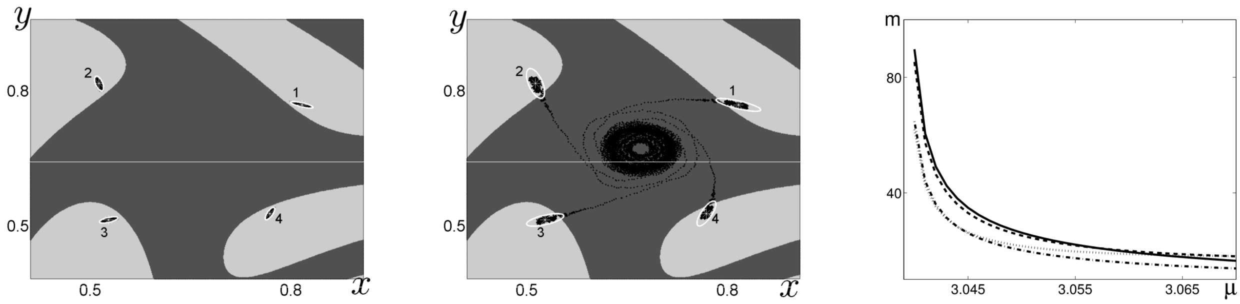

Figure 5: Noise-induced transitions in system (6) with $\beta = 0.49$, $\mu = 3.04$: random states, basins of attraction and confidence ellipses for $\varepsilon = 0.0005$ (a), and $\varepsilon = 0.001$ (b); c) Stochastically forced 4-cycle of system with $\beta = 0.49$: largest eigenvalues of stochastic sensitivity matrices for numbered elements of 4-cycle: solid line (1), dashed line (2), dotted line (3), dash-dotted line (4).

Consider now the system (6) for $\mu = 3.06$ with coexisting 4-cycle and a closed invariant curve. The stochastic sensitivity functions technique for the analysis of closed invariant curves elaborated in [5].

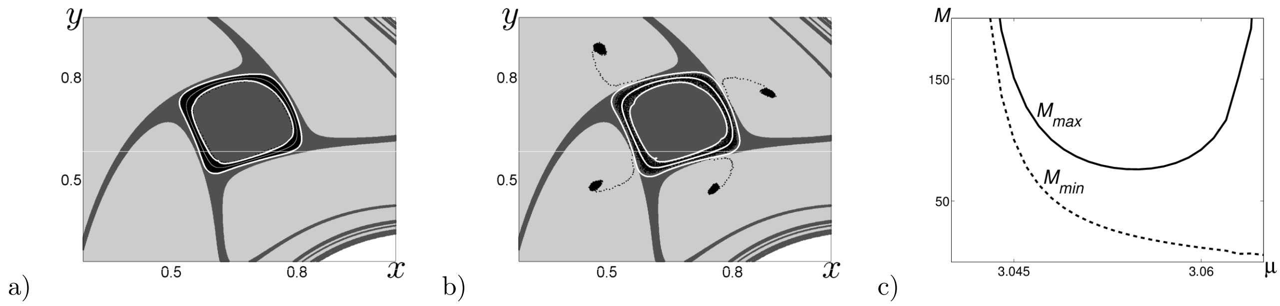

Figure 6: Noise-induced transitions in system (6) with $\beta = 0.49$, $\mu = 3.06$: random states, basins of attraction and confidence ellipses for $\varepsilon = 0.0008$ (a), $\varepsilon = 0.0012$ (b); stochastic sensitivity factors of closed invariant curves (c).

In Fig. 6ab, the deterministic closed invariant curve of system (2) with $\mu = 3.06$ are plotted by white curve, random states of the stochastic system (6) with $\beta = 0.49$ and noise intensities $\varepsilon = 0.0008$ and $\varepsilon = 0.0012$ are plotted by dots. It can be noted that the dispersion of random states along the curve is non-uniform. There are four parts of the random states bundle where a dispersion is much more than on others parts. This non-uniformity agrees well with the peaks of the function $m(\varphi)$. On the base of the stochastic sensitivity function $m(\varphi)$, one can construct confidence bands around the closed invariant curves. In Fig. 6ab, confidence bands are plotted along with random states. As can be seen these bands well reflect a dispersion of random states. In Fig. 6ab, we plot basins of attraction of the closed invariant curve (dark grey) and 4-cycle (light grey). When noise is weak, the confidence band is completely contained in the basin of attraction of the closed invariant curve, and transitions are not induced (see Fig. 6a). With increasing noise, deviations of random states from the closed invariant curve increase too, the confidence band expands and starts to occupy points of the basin of attraction of 4-cycle. As a result, noise-induced transitions to 4-cycle occur (see Fig. 6b).

In Fig. 6c, extremum values $M_{max} = \max m(\varphi)$, $M_{min} = \min m(\varphi)$ of the stochastic sensitivity function are plotted versus parameter μ for $\beta = 0.49$. As one can see, a difference $M_{max} - M_{min}$ that characterizes an overfall of the dispersion along the closed invariant curve, grows with increasing μ.

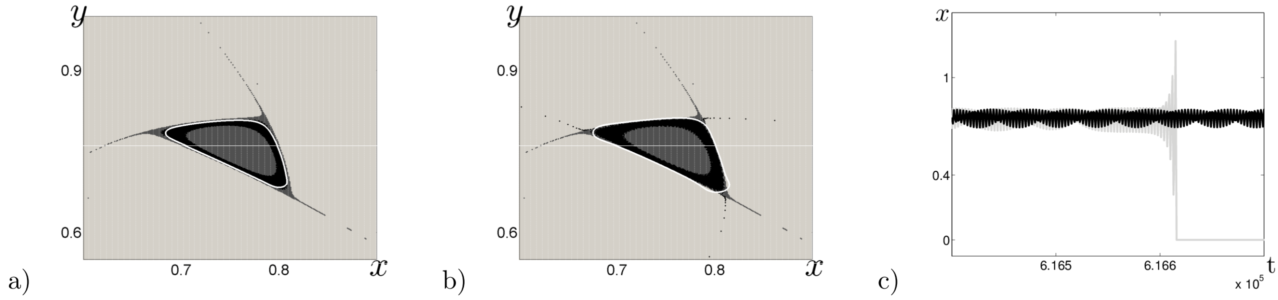

Figure 7: Noise-induced transitions in system (6) with $\beta = 0.32$, $\mu = 4.129$: random states, basins of attraction and confidence bands for $\varepsilon = 0.0001$ (a), $\varepsilon = 0.0002$ (b); corresponding time series for $\varepsilon = 0.0001$ (black), and $\varepsilon = 0.0002$ (grey).

Consider noise-induced transitions in stochastic system (6) with $\beta = 0.32$ in zones of the monostability (existing a closed invariant curve).

In Fig. 7ab, we plot basins of attraction of the closed invariant curve (dark grey) and infinity (light grey), random states of the stochastic system with $\beta = 0.32$ and noise intensities $\varepsilon = 0.0001$ and $\varepsilon = 0.0002$ and also confidence bands. When the starting point belongs to the basin of attraction of infinity, the solutions of the system (6) converge to $-\infty$. When noise is weak, the confidence band is completely contained in the basin of attraction of the closed invariant curve, and transitions are not induced (see Fig. 7a). With increasing noise, deviations of random states from the closed invariant curve increase too, the confidence band expands and starts to occupy points of the basin of attraction of infinity. As a result, noise-induced transitions to infinity (see Fig. 7b). For the illustration of this transition, typical time series are shown in Fig. 7c.

In conclusion, we can summarize that the proposed semi-analytical approach based on the analysis of the mutual arrangement of attractors, their basins of attraction, and confidence domains, is in a good agreement with the results of the direct numerical simulation. In present paper, this approach was illustrated by analyzing noise-induced transitions between equilibrium, 4-cycle, and closed invariant curve, in the logistic-type model. However, our approach is versatile, and can be effectively used in the analysis of stochastic phenomena in more general systems.

Acknowledgments

The work was supported by Russian Science Foundation (N 16-11-10098).

References

[1] V. S. Anishchenko, V. V. Astakhov, A. B. Neiman, T. E. Vadivasova, L. Schimansky-Geier. *Nonlinear Dynamics of Chaotic and Stochastic Systems. Tutorial and Modern Development.* Springer-Verlag, Berlin, Heidelberg, 2007.

[2] L. Arnold. *Random Dynamical Systems.* Springer, Berlin, 1998.

[3] S. Banerjee, R. Parthasarathy. A q-deformed logistic map and its implications. *Journal of Physics A – Mathematical and Theoretical*, 44: 045104, 2011.

[4] I. Bashkirtseva, L. Ryashko, I. Tsvetkov. Sensitivity analysis of stochastic equilibria and cycles for the discrete dynamic systems. *Dynamics of Continuous, Discrete and Impulsive Systems, Series A: Mathematical Analysis*, 17: 501–515, 2010.

[5] I. Bashkirtseva, L. Ryashko. Stochastic sensitivity of the closed invariant curves for discrete-time systems. *Physica A: Statistical Mechanics and its Applications*, 410: 236–243, 2014.

[6] I. Bashkirtseva, E. Ekaterinchuk, L. Ryashko. Attractors of randomly forced logistic model with delay: stochastic sensitivity and noise-induced transitions. *Journal of Difference Equations and Applications*, 22(3): 376–390, 2016.

[7] J.P. Crutchfield, J. Farmer, B.A. Huberman. Fluctation and simple chaotic dynamics. *Phys. Rep.*, 92: 45–82, 1982.

[8] J. B. Gao, S. K. Hwang, J. M. Liu. When can noise induce chaos? *Phys. Rev. Lett.*, 82: 1132–1135, 1999.

[9] L. Gardini, R. Abraham, R.J. Record, D. Fournier-Prunaret. A double logistic map. *Int. J. Bifurcation and Chaos*, 4: 145–176, 1994.

[10] F. Gassmann. Noise-induced chaos-order transitions. Phys. Rev. E., 55: 2215–2221, 1997.

[11] W. Horsthemke, R. Lefever. *Noise-Induced Transitions.* Springer, Berlin, 1984.

[12] J. Inoue, S. Doi, S. Kumagai. Numerical analysis of spectra of the Frobenius-Perron operator of a noisy one-dimensional mapping: toward a theory of stochastic bifurcations. *Phys. Rev. E.*, 64: 056219, 2001.

[13] Yu.A. Kuznetsov, *Elements of Applied Bifurcation Theory*, Springer, 2004.

[14] A. Lasota, M.C. Mackey. *Chaos, Fractals, and Noise: Stochastic Aspects of Dynamics.* Springer, 1994.

[15] Yu. Maistrenko, V. Maistrenko, A. Popovich, E. Mosekilde. Transverse instability and riddled basins in a system of two coupled logistic maps. Phys. Rev. E, 57: 2713–2724, 1998.

[16] M. D. McDonnell, N. G. Stocks, C. E. M. Pearce, D. Abbott. *Stochastic Resonance: From Suprathreshold Stochastic Resonance to Stochastic Signal Quantization.* Cambridge University Press, 2008.

[17] R. May. Simple mathematical models with very complicated dynamics. *Nature*, 261: 459–467, 1976.

[18] R.M. May. Chaos and the dynamics of biological populations. *Proc. R. Soc. Lond. A*, 413: 27–44, 1987.

[19] G. Mayer-Kress, H. Haken. The influence of noise on the logistic model. *J. Stat. Phys.*, 29: 149–171, 1981.

[20] H. Qiu, W. Deng. Optimal harvesting of a stochastic delay logistic model with Levy jumps. *Journal of Physics A – Mathematical and Theoretical*, 49: 405601, 2016.

[21] T.D. Rogers, B.L. Clarke. A continuous planar map with many periodic points. *Journal Applied Mathematics and Computation*, 8: 17–33, 1981.

[22] H.G. Schuster. *Deterministic Chaos. An Introduction.* Weinheim, Physik-Verlag, 1984.

[23] J. Maynard Smith. *Mathematical Ideas in Biology.* Cambridge University Press, 1968.

[24] J.R. Pounder, T.D. Rogers. The geometry of chaos: Dynamics of a nonlinear second-order difference equation. *Bulletin of Mathematical Biology*, 42: 551–597, 1980.

[25] R. Sacker. *On invariant surfaces and bifurcation of periodic solutions of ordinary differential equations.* Report IMM-NYU 333, New York University, 1964.

[26] G. Tanaka, M. Sanjuan, K. Aihara. Crisis-induced intermittency in two coupled chaotic maps: Towards understanding chaotic itinerancy. *Phys. Rev. E*, 71: 016219, 2005.